MOLECULAR AND CELLULAR BIOLOGY, Sept. 2006, p. 6713–6726 Vol. 26, No. 17
0270-7306/06/$08.00+0 doi:10.1128/MCB.00296-06

Mutation of the Murine Bloom's Syndrome Gene Produces Global Genome Destabilization

Nicholas Chester,* Holger Babbe, Jan Pinkas,† Charlene Manning,‡ and Philip Leder

Department of Genetics, Harvard Medical School, 356 New Research Building, 77 Avenue Louis Pasteur, Boston, Massachusetts 02115

Received 16 February 2006/Returned for modification 16 March 2006/Accepted 15 June 2006

Bloom's syndrome (BS) is a genetic disorder characterized cellularly by increases in sister chromatid exchanges (SCEs) and numbers of micronuclei. BS is caused by mutation in the *BLM* DNA helicase gene and involves a greatly enhanced risk of developing the range of malignancies seen in the general population. With a mouse model for the disease, we set out to determine the relationship between genomic instability and neoplasia. We used a novel two-step analysis to investigate a panel of eight cell lines developed from mammary tumors that appeared in *Blm* conditional knockout mice. First, the panel of cell lines was examined for instability. High numbers of SCEs were uniformly seen in members of the panel, and several lines produced chromosomal instability (CIN) manifested by high numbers of chromosomal structural aberrations (CAs) and chromosome missegregation events. Second, to see if *Blm* mutation was responsible for the CIN, time-dependent analysis was conducted on a tumor line harboring a functional floxed *Blm* allele. The floxed allele was deleted in vitro, and mutant as well as control subclones were cultured for 100 passages. By passage 100, six of nine mutant subclones had acquired high CIN. Nine mutant subclones produced 50-fold more CAs than did nine control subclones. Finally, chromosome loss preceded the appearance of CIN, suggesting that this loss provides a potential mechanism for the induction of instability in mutant subclones. Such aneuploidy or CIN is a universal feature of neoplasia but has an uncertain function in oncogenesis. Our results show that *Blm* gene mutation produces this instability, strengthening a role for CIN in the development of human cancer.

Bloom's syndrome (BS) is a rare recessive genetic disorder characterized by proportional dwarfism, telangiectatic erythema, immune deficiency, and a greatly enhanced risk for most cancers (18). The elevated cancer risk is manifested by increased and early appearance of leukemias, lymphomas, rare tumors, and carcinomas, with a mean age of onset of 25 years (20).

The gene for Bloom's syndrome (*BLM*) encodes a member of the RecQ family of helicases (14). In humans, there are five RecQ members including WRN, and RECQ4, mutations in which give rise to Werner's and Rothmund-Thomson syndromes, respectively (2). RecQ family members have been identified in most multi- and single-cell organisms examined to date, including *Xenopus*, *Drosophila*, *Gallus*, *Caenorhabditis elegans*, *Saccharomyces cerevisiae*, *Schizosaccharomyces pombe*, and *Escherichia coli* (2). Biochemical analysis has shown that RecQ members, including WRN and BLM, are ATP-dependent DNA helicases that possess a 3′-5′ unwinding activity with different substrate specificities (2).

A unique feature of the disease is pairing between homologous chromosomes and high numbers of sister chromatid exchanges (SCEs) seen in cultured BS cells treated with bromodeoxyuridine (5, 18, 24, 46). Further evidence that BLM suppresses hyperrecombination comes from in vitro assays where the helicase interacts with TOPIIIα and cooperates with the strand cleavage and unwinding activities of this type I topoisomerase to resolve a double Holliday junction structure, suppressing exchanges between flanking DNA sequences (56, 57). Replication defects have been identified in BS cells, where chain elongation during DNA synthesis proceeds at a lower rate than in normal cells and where there is an accumulation of abnormal replication intermediates (22, 36). In addition, cells bearing an impaired BLM mutant protein fail to undergo normal cell cycle progression after release from hydroxyurea-induced S-phase arrest (9).

Much research has been conducted to identify the unique defects that BS cells produce that contribute to the 100-fold-increased risk of cancer seen in the disease (4). BS cells have increased numbers of spontaneous chromosome gaps, breaks, and rearrangements (17, 51). Increased somatic mutation has been found in cultured fibroblasts and lymphocytes in vivo, where the frequency of mutation at the hypoxanthine phosphoribosyltransferase locus is increased 8- to 10-fold (53, 55). It has been proposed that the difference in neoplastic potential between a normal cell and a Bloom's syndrome cell is a higher mutation rate and loss of heterozygosity (LOH) provided by hyperrecombination (18, 21). However, it is not known to what extent gene mutation drives neoplasia in Bloom's syndrome or in the general population.

An alternative model proposes that aneuploidy and chromosomal instability (CIN) drive cancer (12, 43, 48). Likewise, the potential for BS cells producing CIN has been evaluated, and in vitro inactivation of *BLM* in a human colorectal cancer line produced no gross structural rearrangements or chromosome missegregation in this study (52). Yet, little is known about the

* Corresponding author. Mailing address: Department of Genetics, Harvard Medical School, 356 New Research Building, 77 Avenue Louis Pasteur, Boston, MA 02115. Phone: (617) 432-7578. Fax: (617) 432-7663. E-mail: nchester@rascal.med.harvard.edu.

† Present address: Amgen, One Kendall Square, Cambridge, MA 02139.

‡ Present address: Genzyme Corporation, 5 Mountain Road, Framingham, MA 01701.

mutagenic potential of micronuclei (MN) seen in BS cells. Increased numbers of micronuclei have been detected in exfoliated cells from BS patients relative to controls (45). Cultured BS fibroblasts expel micronuclei during S phase, and these contain bromodeoxyuridine and replication protein A, reflecting failed DNA replication events (58). Moreover, chromosome loss has been documented in peripheral lymphocytes from BS individuals, likely resulting from production of micronuclei (1, 49).

In order to better understand how mutation in human *BLM* produces genetic instability that in turn induces neoplasia, we made a panel of cell lines from mammary tumors occurring in Bloom's syndrome gene conditional knockout (CKO) mice. As expected, panel lines generated high numbers of SCEs. However, at least several members of the panel exhibited CIN characterized by chromosome missegregation and high numbers of chromosomal structural abnormalities. By employing a unique two-step approach to the analysis of the cell lines, we show that the *Blm* gene mutation is responsible for producing this instability. Further, the data implicate *Blm* mutation-induced chromosome loss in the subsequent appearance of CIN. Last, we analyzed the DNA contents of mammary tumors that appeared in different cohorts of Bloom's syndrome CKO mice and found evidence for CIN occurring in the form of aneuploidy in vivo.

MATERIALS AND METHODS

Construction of a *Blm* exon 8 conditional allele in ES cells and mice. Embryonic stem (ES) clones containing one copy of the $Blm^{tm2Ches}$ allele (Fig. 1C) have been made previously, and one was used in a transient transfection assay with a Cre-expressing plasmid to generate conditional allele $Blm^{tm4Ches}$. Following plating of cells under limiting dilution, colony formation, and propagation in parallel wells in the presence and absence of G418, genomic DNA from drug sensitive clones was analyzed by PCR and Southern blot assay to identify clones that contained *loxP* sites flanking exon 8 (Fig. 1B). PCR primers 1 and 2, used to verify the presence of the 5′ site, have been described previously (Fig. 1C) (39). Analysis of clone genomic DNA for the presence of the 3′ site was done by PCR with sense primer 3 (5′-TCTACTGCTCAGTAAAGGCTC-3′) and antisense primers 4 and 5 (5′-CCGATATCAAGCTTAGGATCC-3′ and 5′-ATTTAGGC TTCCATTCTGAGG-3′, respectively) under previously described conditions (7). Microinjection of 129 SvEv ES cells bearing the exon 8 floxed $Blm^{tm4Ches}$ allele into blastocysts and production of heterozygous agouti mice were done using standard techniques (7).

Generation of $Blm^{tm4Ches/tm4ches}$ homozygous floxed and CKO mice. Intercrosses between $Blm^{+tm4Ches}$ heterozygotes produced a mouse cohort that was homozygous for the floxed allele. Genotype assay for mouse strains was performed by PCR with primers 1 and 2 (Fig. 1B; floxed allele), sense Cre5N (5′-TCGACCAGGTTCGTTCACTCATGG-3′) and antisense Cre3N (5′-CAG GCTAAGTGCCTTCTCTACACC-3′) (*cre* transgene), and three primers specific to the original *tm1Ches* allele (7). Floxed allele deletion analysis was performed by Southern blot assay with a *Blm* exon 9-containing probe on Hind-III digested genomic DNA from normal mouse tissues, tumors, and tumor cell lines (Fig. 2) (39).

Cell culture and soft agar growth assay. Tumor tissue from CKO animals was diced with a razor blade under sterile conditions and plated in Dulbecco's modified Eagle's medium supplemented with 10% fetal calf serum, 2 mM glutamine, 100 units/ml penicillin, and 100 μg/ml streptomycin in six-well dishes. After multiple medium changes and recovery from senescence (typically 2 to 3 months), cells were trypsinized, counted, and plated at low density in 15-cm dishes. Two to 3 weeks later, colonies were picked and expanded. Single-cell clonal lines were established in 10-cm dishes and propagated by the 3T3 protocol (23). Growth in soft agar was by bilayer assay, with the bottom plating and top cell layers containing 0.6% and 0.4% agar (Noble agar; DIFCO), respectively. A total of 10^5 cells were plated in triplicate in complete medium in 60-mm dishes and allowed to grow for 3 weeks. Visualization of colonies was enhanced by overnight incubation in 100 μg/ml tetrazolium violet in medium (iodonitrotetrazolium chloride; Sigma). Colonies 200 μm or greater in diameter were scored manually under a dissecting microscope with the aid of a grid.

Purification of recombinant Cre protein and in vitro deletion of *Blm* exon 8. TUNER(DE3)pLacI(Novagen)pTriEx(Novagen)-His-TAT-NLS-Cre (HTNC) bacteria were grown, induced, and lysed, and recombinant protein was purified from extract on an Ni nitrilotriacetic acid agarose (QIAGEN) column, dialyzed, and stored as described previously (40). Deletion of floxed *Blm* exon 8 in line 1690-12 (passage 4) was by addition of 300 μg of HTNC protein in complete medium onto 1×10^5 cells for 4 h. This was followed by a phosphate-buffered saline (PBS) wash, addition of complete medium, and recovery for a day. Cells were then trypsinized, counted, and plated at low density for cloning and expansion to cell lines. Assay for rearrangement was initially by PCR and later by Southern blotting on genomic DNA. Deletion of exon 8 in lines U-10 (passage 49 [p49]), U-23 (p49), and 9258-5 (p5) and production of subclones for chromosome loss analysis were performed in a similar manner as for line 1690-12 (see above), except parallel cultures were treated with buffer to generate control subclones. For the three lines and control NIH 3T3 cells, 15 mutant p4 to p6 subclones were compared to 15 control p4 to p6 subclones, with 10 metaphases scored per subclone for a total of 300 metaphase per line.

Sister chromatid exchange assay. Sister chromatid exchange assay was performed as described previously (19) with the following modification: images of differentially stained chromosomes were visualized with a UV source, a DAPI (4′,6′-diamidino-2-phenylindole) filter with a 100× objective and were captured with a SPOT version 2.3 digital camera (Diagnostic Instruments) after staining of metaphase spotted slides with Hoechst 33258 dye (Molecular Probes) in distilled water at a concentration of 250 ng/ml for 15 min. Computer printouts of metaphase images were scored manually for SCEs and chromosome number.

Chromosome number and structural abnormality assay. Preparation, spotting, and Giemsa staining of metaphases were performed as described previously (19). Two types of abnormalities were scored, i.e., metacentric end-to-end fusions, containing a characteristic constriction in the length of the chromosome, and small marker chromosomes, defined here as being smaller than the smallest consistently sized chromosomes. The smallest mouse chromosome (number 19) is approximately 30% of the size of the largest chromosomes (numbers 1 and 2). Visualization was with a 63× or 100× objective, with image capture and scoring as described above.

Micronucleus assay. Assay for micronucleus frequency was performed on cells grown on microscope slides in 10-cm dishes to subconfluent or just-confluent density. Harvest was by PBS washing, fixation for 5 min in 10% buffered formalin (VWR), PBS washing, H_2O washing, and air drying. Visualization was with DAPI-containing coverslip mounting medium (Vector) and UV microscopy with a 40× objective. Only extranuclear bodies free of and no larger than one-third the size of the main nucleus were scored. Cells with single or multiple micronuclei were both scored as one.

Anaphase laggard assay. Cells were arrested in mitosis by addition of 2 μM nocodazole (CalBiochem) in complete medium for 3 h. Drug-containing medium was removed, and cells were washed twice, replenished with complete medium, and incubated for 2 h following release to allow progression into anaphase. Cell harvest and UV microscopy were as for the micronucleus assay (see above). Only unattached chromosomal material free of microtubule-attached segregating chromosomes was scored; bridges were not included in the assay.

Fluorescence-activated cell sorter analysis of tumor cell nuclei. Preparation of nuclei from 50-μm sections of fixed mammary tumor samples embedded in paraffin blocks was performed as described previously (11). Nuclei were resuspended at 1×10^6/ml in PBS, digested with RNase A for 1 h, stained with propidium iodide, and subjected to flow cytometric analysis (FACSCalibur; Becton Dickinson). Tumor samples and normal organ diploid controls (spleen, liver, and lung) obtained from paraffin blocks from the same mouse were compared to assay for DNA content shifts, with the control samples being used to establish the position of the G_0/G_1 peak. The minimum detectable DNA index as a function of the coefficient of variation was determined as previously described (42). To insure reproducibility, all tumor samples and controls were assayed two or three times with fresh preparations of nuclei.

Statistics. Standard deviations from the mean and *P* values from the Student *t* test (two sided with unequal variance) were generated using computer software.

RESULTS

Generation of a *Blm* conditional allele in ES cells and mice. In order to better understand the mechanism of Bloom's syndrome-induced malignancy, we needed to create appropriate mouse models. Two previous mouse Bloom's syndrome gene

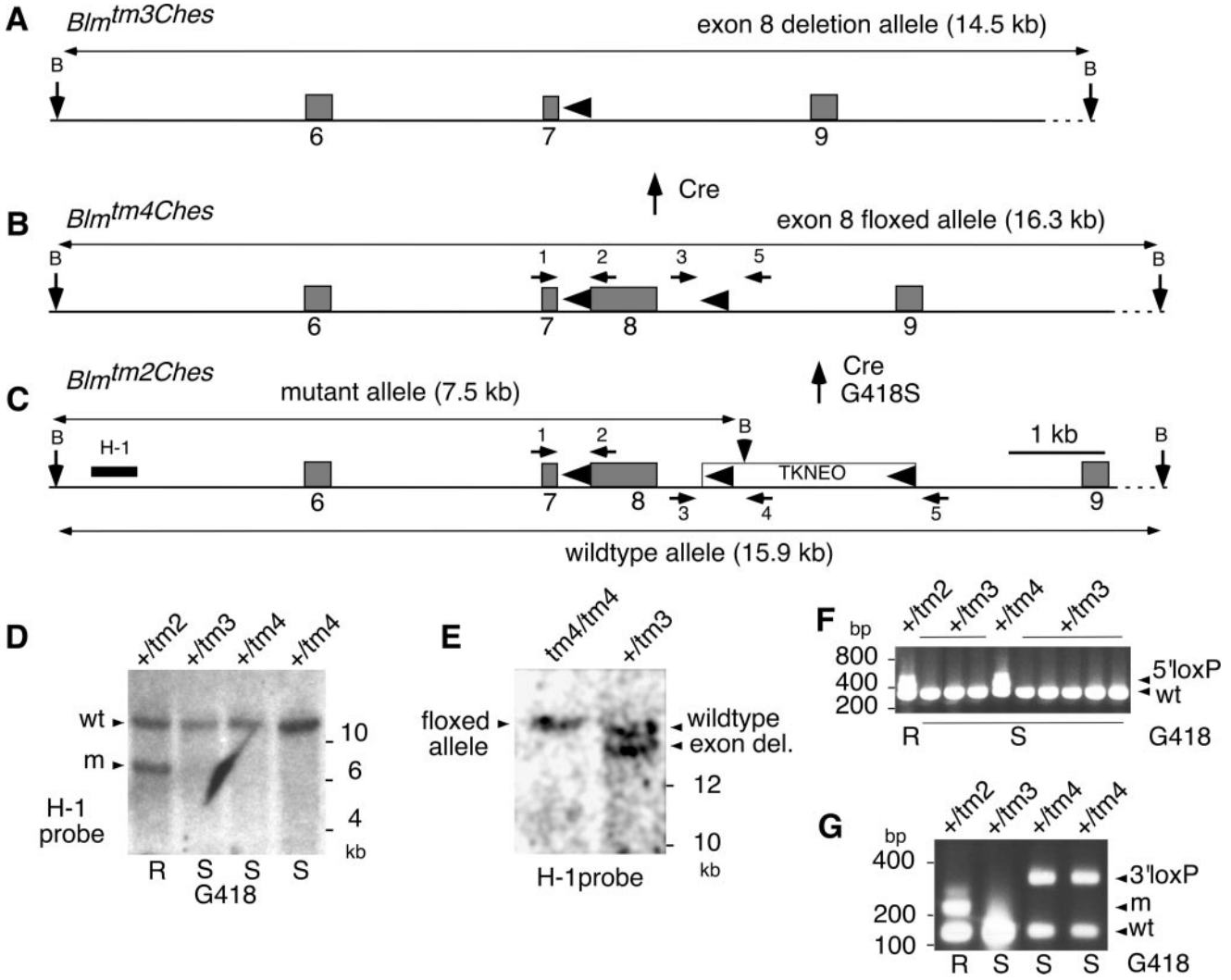

FIG. 1. Conditional targeted disruption of the mouse *Blm* gene. (A) The null $Blm^{tm3Ches}$ allele was produced in vivo from the conditional $Blm^{tm4Ches}$ allele following Cre-mediated deletion of exon 8. (B and C) The conditional $Blm^{tm4Ches}$ allele was made from ES cells harboring the parental $Blm^{tm2Ches}$ allele and had *Blm* exon 8 flanked by a single 5′ *loxP* site and a 3′ floxed *TKNEO* drug resistance cassette. This was by addition of a Cre-expressing plasmid and a G418 sensitivity screen for single-cell clones that had lost the *TKNEO* cassette while retaining exon 8. (D) Southern blot analysis on genomic DNA shows that the mutant (m) 7.5-kb BamHI fragment is lost in G418-sensitive (S) clones, while it is present in the $Blm^{tm2Ches}$ drug-resistant (R) parental clone. DNA probe H-1 is indicated in panel C (black bar). (E) Southern blot analysis of BamHI-digested mouse tail DNAs probed with H-1 DNA shows a single 16.3-kb floxed (*tm4*/*tm4*) allele band in lane 1, and the 14.5-kb exon 8 deletion and 15.9-kb wild-type allele bands are seen in heterozygote (+/*tm3*) DNA in lane 2. (F) Primers 1 and 2 (B and C) amplified the exon 8 5′ *loxP* site 432-bp product from $Blm^{tm2Ches}$ R parental clone DNA and two S clones, one of which is shown. (G) To confirm that the 3′ *loxP* site was retained, DNA from the two 5′ *loxP* site-bearing S clones was amplified with the simultaneous addition of primers 3, 4, and 5 and produced, in each case, a 318-bp product in addition to the 136-bp wild-type allele product. In contrast, $Blm^{tm3Ches}$ DNA yielded only the wild-type allele due to deletion of all three primer binding sites, and $Blm^{tm2Ches}$ parental clone DNA produced a 233-bp drug resistance cassette product arising from primers 3 and 4. Clones with *loxP* sites flanking exon 8 ("floxed") were designated allele $Blm^{tm4Ches}$ (B). B, BamHI restriction site; dashed line, genomic region (not drawn to scale); *TKNEO*, *PGKtkneo* dicistronic drug resistance cassette; black triangles, *loxP* sites; +/*tm2*, $Blm^{+/tm2Ches}$; +/*tm3*, $Blm^{+/tm3Ches}$ allele; +/*tm4*, $Blm^{+/tm4Ches}$ allele; m, mutant; wt, wild type.

mutant alleles constructed in our laboratory have resulted in embryonic lethality. The first allele, $Blm^{tm1Ches}$, contained the neomycin drug resistance cassette (*neo*) in exon 8 as the result of a simultaneous insertion/deletion event (7). The second allele, $Blm^{tm3Ches}$, contained an exon 8 deletion that resulted in a frameshift mutation and a stop codon (Fig. 1A) (39). We then constructed a conditional third allele, $Blm^{tm4Ches}$ with *loxP* sites, which flanked ("floxed") exon 8 (Fig. 1B). ES cells from one clone bearing the floxed allele were used to generate a homozygous mouse strain.

Production of mammary tumors and cell lines from *Blm* CKO mice. One of our Bloom's syndrome CKO strains of mice utilized a heat shock promoter to drive Cre expression in vivo. The *Hs-cre*-expressing mouse line produces widespread deletion of floxed reporter alleles in a variety of tissues both in embryos and adult mice (10). CKO $Blm^{tm1Ches/tm4Ches}$; *Hs-cre*

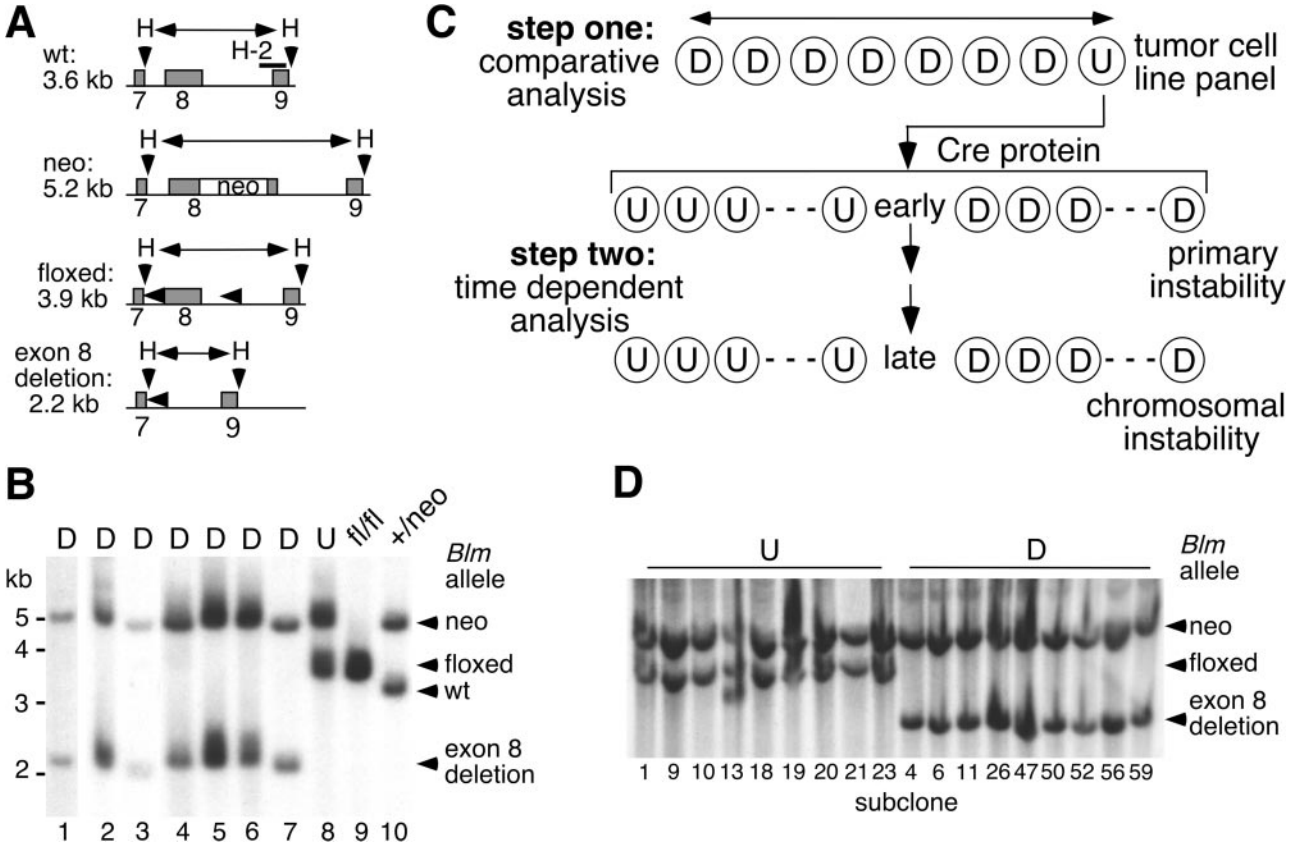

FIG. 2. Assay for deletion of the *Blm* floxed allele in tumor lines by Southern blot analysis and scheme of the two-step protocol performed on the tumor cell line panel. Tumor-bearing mice have one copy each of the *tm1Ches* (*neo*) and *tm4Ches* (floxed) alleles in addition to a *cre* transgene. (A) Predicted sizes of the four *Blm* alleles with HindIII (H)-digested DNA. *Blm* exons 7, 8, and 9 are shown as numbered gray boxes. *neo*, *PGKneo* cassette; black triangles, *loxP* sites; wt, wild type. (B) Southern blot analysis of DNA from cloned tumor cell lines was performed using probe H-2 (black bar). Lanes 1 to 7 identify cell lines that produced the exon 8 deletion (D); in contrast, lane 8 cell line had an undeleted floxed allele (U). Control floxed/floxed (fl/fl) and *neo* cassette (+/*neo*)-containing mouse embryonic fibroblast genomic DNAs are shown in lanes 9 and 10, respectively. Lanes and cell lines: 1,1579-5; 2,1578-2; 3, 9261-9; 4, 9354-14; 5, 1780-11; 6, 1776-4; 7, 1795-2; 8, 1690-12. (C) Rationale for two-step analysis of the tumor cell line panel. In step one, comparative analysis was performed on the eight cell lines in parallel at similar passage numbers. In step two, the floxed allele control (U) cell line was employed for time-dependent analysis by generating deleted (D) mutant and matched undeleted (U) control subclones by using Cre protein transduction into cultured cells. Subclones were passaged and assayed at early and late times in their culture histories to identify mutant (D) cultures that developed chromosomal instability in addition to the primary instability. (D) Southern blot analysis of subclone DNAs harvested at the end of the experiment from passage 97 to 101. Nine control (U) subclones with an intact floxed allele are shown in parallel with nine mutant (D) subclones that harbored the exon 8 deletion. Subclone number designations are indicated at the bottom.

mice bearing one null and one floxed allele in addition to the *cre* transgene were generated. In the *Blm Hs-cre* cohort, 61 animals were maintained up to 2 years of age to monitor for tumor development. Interestingly, mammary tumors developed in 7 of 12 female CKO mice between 10 and 24 months of age. This was significantly different from the 1 out of 20 female non-CKO animals that developed mammary tumors ($P = 0.005$). The *Blm* CKO animals, which are mosaics of heterozygote and null cells, produced the same mammary myoepithelial tumors as those found in *Blm* hypomorphs (39). A second, less tumorigenic prostate-specific antigen promoter-*cre* transgene (*PSA-cre*) cohort produced mammary adenomyoepitheliomas in 2 of 23 female CKO mice. Although none were seen in 16 non-CKO female mice at 2 years of age, this difference was not significant ($P = 0.16$). Few additional tumors were seen in either cohort or sex, and this may reflect low levels and variable excision of the floxed allele as assayed by Southern blotting on various organs from CKO animals (data not shown). Last, a third tumor cohort bearing the ovine beta-lactoglobulin promoter-*cre* transgene (*BLG-cre*) was analyzed. The milk protein promoter directs Cre activity to female mouse mammary epithelial cells during lactation (47). Multiparous *Blm BLG-cre* mice were followed for tumor development up to 21 months of age. Mammary tumors developed in 7 of 25 CKO mice aged 13 to 19 months. This was significantly more than the one tumor that appeared among 27 non-CKO control mice ($P = 0.019$). In contrast to the appearance of mammary adenomyoepitheliomas in the *Hs-cre* and *PSA-cre* cohorts, *BLG-cre* mice produced mainly adenocarcinomas (Table 1). To assess whether deletion of exon 8 occurred in vivo, tumor sample nuclei (used for DNA content analysis [see Materials and Methods]) were subjected to PCR with primers to the floxed allele. We found that all the mammary tumor samples from the three cohorts showed partial or complete deletion

TABLE 1. DNA contents of mammary tumors occurring in three cohorts of *Blm* conditional knockout mice

Cohort and mouse	Genotype	Tumor type	DI[a]	CV[b]	DNA ploidy[c]	Cell line stability[d]
Hs-cre						
1578	CKO	Adenomyoepithelioma	1.1	13	Diploid	Unstable
1579	CKO	Adenomyoepithelioma	1.0	10	Diploid	Unstable
1780	CKO	Adenomyoepithelioma	0.9	10	Diploid	Moderate
1795	CKO	Adenomyoepithelioma	0.9	12	Diploid	Stable
1776	CKO	Adenomyoepithelioma	1.0	10	Diploid	Stable
1690	CKO	Adenomyoepithelioma	0.9	8	Diploid	Stable
9907	CKO	Fibroadenoma	1.8, 3.4	8, 8	Aneuploid	NA[f]
PSA-cre						
9261	CKO	Adenomyoepithelioma	0.9	8	Diploid	Unstable
9354	CKO	Mixture[e]	1.6	8	Aneuploid	Moderate
BLG-cre						
1852	CKO	Adenocarcinoma	1.4, 1.7	5, 8	Aneuploid	NA
7877	CKO	Adenocarcinoma	1.3, 2.0	4, 8	Aneuploid	NA
1983	CKO	Adenocarcinoma	1.2	5	Hyperdiploid	NA
7725	CKO	Adenocarcinoma	1.2	5	Hyperdiploid	NA
7885	CKO	Squamous cell carcinoma	1.1	4	Hyperdiploid	NA
7852	CKO	Ductal carcinoma in situ	1.3	4	Hyperdiploid	NA
7724	CKO	Adenocarcinoma	1.0	6	Diploid	NA
1980	Reporter[g]	Adenocarcinoma	2.5	4	Aneuploid	NA

[a] DI, DNA index. Two values refer to two different stem lines.
[b] CV, coefficient of variation. Two values refer to two different stem lines.
[c] Tumors were defined as diploid if control organ and tumor G_0/G_1 DNA content peaks determined by flow cytometry were ≤10% of each other, hyperdiploid if there was a positive shift of 10 to 20%, and aneuploid if there was a shift of ≥ 30%. The minimum detectable DI as a function of the CV was established for each sample-control pair as described by Rabinovitch (42).
[d] From Results and Fig. 3.
[e] The mouse had multiple tumors, all of which were a mixture of adenocarcinoma, squamous cell carcinoma, and adenomyoepithelioma.
[f] NA, not applicable.
[g] Control bearing one wild-type allele and one *tm4Ches* floxed allele as well as the transgene.

of exon 8, providing additional evidence that the *Blm* mutation induced the tumors (data not shown). Cases where partial deletion was found likely occurred because of contamination of the PCR assay with normal tissue surrounding the tumor.

Confirmation of *Blm* exon 8 deletion in a panel of Bloom's syndrome mammary tumor cell lines. A panel of eight mammary myoepithelial cell lines was assembled by in vitro culture of excised tissue from two and six tumors from the *Blm PSA-cre* and *Blm Hs-cre* cohorts, respectively. We were unable to culture most tumors from the *BLG-cre* cohort. All tumor cell lines used in the study were cloned, and the passage numbers used varied from p8 to p21. As detected by PCR analysis, the floxed allele was entirely deleted in seven of the lines (data not shown). Likewise, by Southern blot assay the same result was confirmed (Fig. 2B, lanes 1 to 7). In contrast, cell line 1690-12, derived from tumor 1690, did not undergo deletion of exon 8, nor did a dozen other clones made from this tumor culture (Fig. 2B, lane 8, and data not shown). Therefore, these clones appear to have arisen from cultured tumor cells bearing an intact conditional allele. Hereafter, "mutant" and "control" refer to deleted and undeleted cell lines, respectively.

A two-step analysis to assay for indirect effects of the *Blm* mutation. Interestingly, several members of the tumor line panel displayed CIN. This finding prompted us to employ a novel two-step protocol to analyze and thus better understand the nature and origin of this instability. In step one, a comparative analysis was performed to determine the range of genomic instability that panel members harbored. Our findings (shown in the next section) did not allow us to determine whether the unanticipated CIN was a consequence of the *Blm* mutation or not. To determine this, we employed a second step by utilizing the undeleted panel member. By adding Cre protein to these cells, we created sets of mutant experimental and control subclones. These were cultured and assayed in a time-dependent manner for the appearance of subclones that had acquired chromosomal instability (Fig. 2C).

Step one: Bloom's syndrome mammary tumor cell lines reveal a wide variation in genomic instability. First, we employed the SCE assay to see if our tumor lines would display the genomic instability characteristic of Bloom's syndrome cells. For the seven mutant lines, values were uniformly high and ranged from (average ± standard deviation) 1.3 ± 0.3 to 1.8 ± 0.32 SCEs/chromosome, indicating the presence of the Bloom's syndrome hyperrecombination phenotype (Fig. 3A). In contrast, the control tumor line, 1690-12, suppressed numbers of SCEs, as did wild-type NIH 3T3 cells, at 0.26 ± 0.15 SCEs/chromosome and 0.28 ± 0.05 SCEs/chromosome, respectively (Fig. 3A).

Next, we performed the micronucleus assay (Fig. 3B), which has been used to demonstrate genomic instability in cells from BS individuals and in nucleated red blood cells from *Blm* null mouse embryos (7, 45). Surprisingly, numbers of micronuclei showed a greater-than-threefold variation among the seven mutant lines, as shown in Fig. 3B and Fig. 4A and B. Lines 1578-2, 9261-9, and 1579-5 showed the highest MN values among panel members, with 34.5 ± 0.7, 28.4 ± 1.1, and 27.7% ± 1.0% micronuclei, respectively. In contrast, line 1795-2 pro-

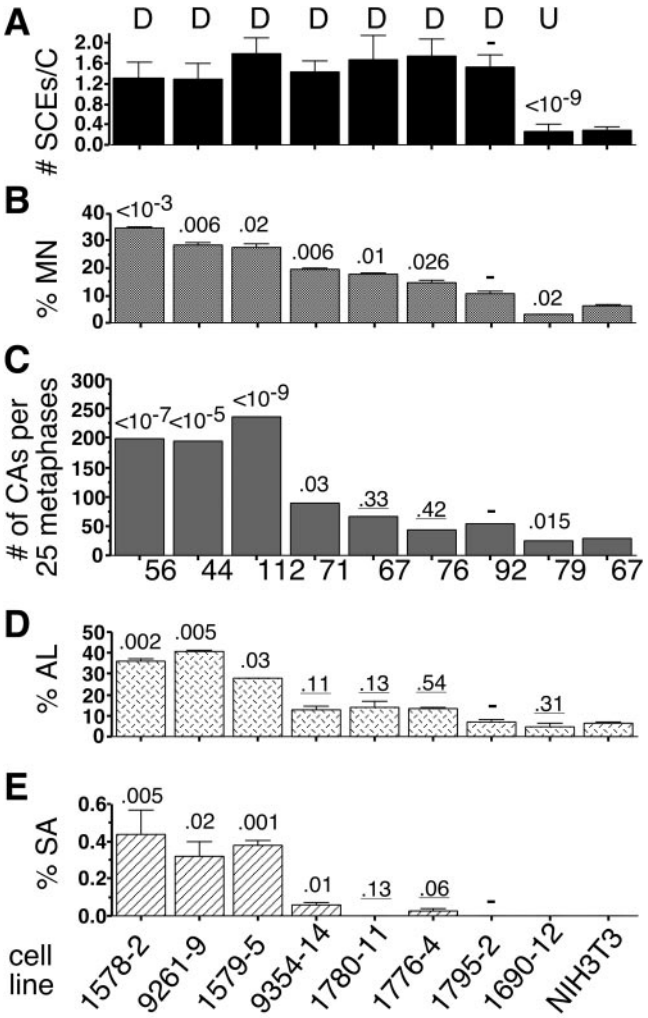

FIG. 3. Comparative analysis of the tumor cell line panel reveals lines that have chromosomal instability. Results from a representative set of experiments are shown, and passage numbers for the lines varied from 15 to 21. For each cell line and for all assays except the SCE assay, samples were taken within one passage number. (A) Sister chromatid exchange assay. Results are expressed as number of SCEs/chromosome (C), with 500 chromosomes scored for each line ($n = 1$). (B) Micronucleus assay. Results are expressed as percent MN for 2×500 cells scored per sample ($n = 3$). (C) Chromosomal aberration assay. Results are expressed as total number of metacentric translocations and small marker chromosomes per 25 metaphases counted per line. Modal chromosome numbers are given at the bottom ($n = 3$). (D) Anaphase laggard assay. Results are expressed as percent AL in cells released from nocodazole arrest, with 2×100 anaphase figures scored per sample ($n = 3$). (E) Soft agar growth assay. Results are expressed as percent input cells that form colonies in soft agar (SA) ($n = 5$). Cell line order is based on the results from the MN assay (B) and is from highest to lowest value, with the NIH 3T3 cell line added last for comparison. Bars show average values (in panels A, B, D, and E). Error bars show standard deviations from the mean. *P* values are shown relative to cell line 1795-2 (dash) in panels A to E, and values that are insignificant ($P \geq 0.05$) are underlined.

duced the lowest MN value in the panel, with 10.7% ± 0.7% micronuclei. Consistent with its production of low numbers of SCEs, control line 1690-12, with 3.0% ± 0.3% MN (Fig. 3B), produced fewer micronuclei than any mutant line.

In addition, the tumor panel was assayed for numbers of chromosomal structural abnormalities. B-lymphoblastoid cell lines established from lymphocytes from BS patients showed greater numbers of chromosomal aberrations (CAs) than seen in control lymphoblastoid cell lines (26). To determine this, we scored two types of structural abnormalities that could be visualized from Giemsa-stained metaphase spreads, i.e., metacentric end-to-end chromosome translocations and abnormally small chromosomes or small marker chromosomes (Fig. 4C). Among panel members, the CA assay showed a greater-than-fivefold variation. The three most unstable lines from the MN assay produced the most structural abnormalities, with 199, 194, and 235 CAs per 25 metaphases for 1578-2, 9261-9, and 1579-5, respectively. In contrast, the two most stable lines by MN assay, 1795-2 and 1776-4, produced fewer abnormalities, with 54 and 44 CAs/25 metaphases, respectively (Fig. 3C). Control line 1690-12 produced the fewest abnormalities, with 25 CAs/25 metaphases (Fig. 3C). Panel members 1780-11 and 9354-14 yielded intermediate values in both the MN and CA assays (Fig. 3B and C).

MN and CA assays indicated a high degree of variation among different mutant cell lines, whereas the SCE assay reported a relatively uniform response for the same lines. The difference in nuclear morphology between lines was striking, where unstable lines produced cells with multiple nuclei, nuclei containing lobes, and nuclei with multiple micronuclei. In contrast, nuclei from stable lines were uniform in size and shape and produced only occasional micronuclei (Fig. 4A and B and data not shown). CIN is a ubiquitous phenomenon in cancer and is defined as the appearance of chromosome missegregation and aneuploidy (12, 35, 43). The higher numbers of micronuclei produced by unstable lines probably arise as a consequence of chromosome missegregation. In support of this, it is known that mutations in genes that produce chromosome segregation defects produce micronuclei. These genes include the tumor suppressors BRCA2 and BRCA1, hCDC4, and BubR1 (3, 8, 44).

To confirm that unstable members of the tumor cell line panel exhibit segregation defects at mitosis, we scored anaphase laggards (AL) in cultures that had been released from nocodazole arrest. Laggards occurring in anaphase are visualized as loose chromosomal material appearing between separating daughter cells (Fig. 4E). As shown in Fig. 3D, scoring analysis of AL produced a sixfold range between unstable and stable lines 9261-9 and 1795-2, which yielded 40.5 ± 0.7 and 7.0% ± 1.4% AL, respectively. Analogous to the results of the MN and CA assays, the other unstable lines, 1578-2 and 1579-5, produced high values of 36.0 ± 1.41 and 28.0% ± 0.0% laggards, respectively. In contrast, the lines with intermediate instability, 9354-14 and 1780-11, and stable line 1776-4 all yielded lower AL values (Fig. 3D). This assay shows directly that unstable panel members produce relatively high levels of chromosome missegregation and confirms that the MN assay measures this as well. Based on comparative analysis of members of the tumor line panel, the results of the genomic instability assays reveal a wide range of numerical and structural chromosomal instability among the lines.

Direct correlation between degree of transformation and level of chromosomal instability in tumor cell lines. We were interested in assessing the role of CIN in producing transfor-

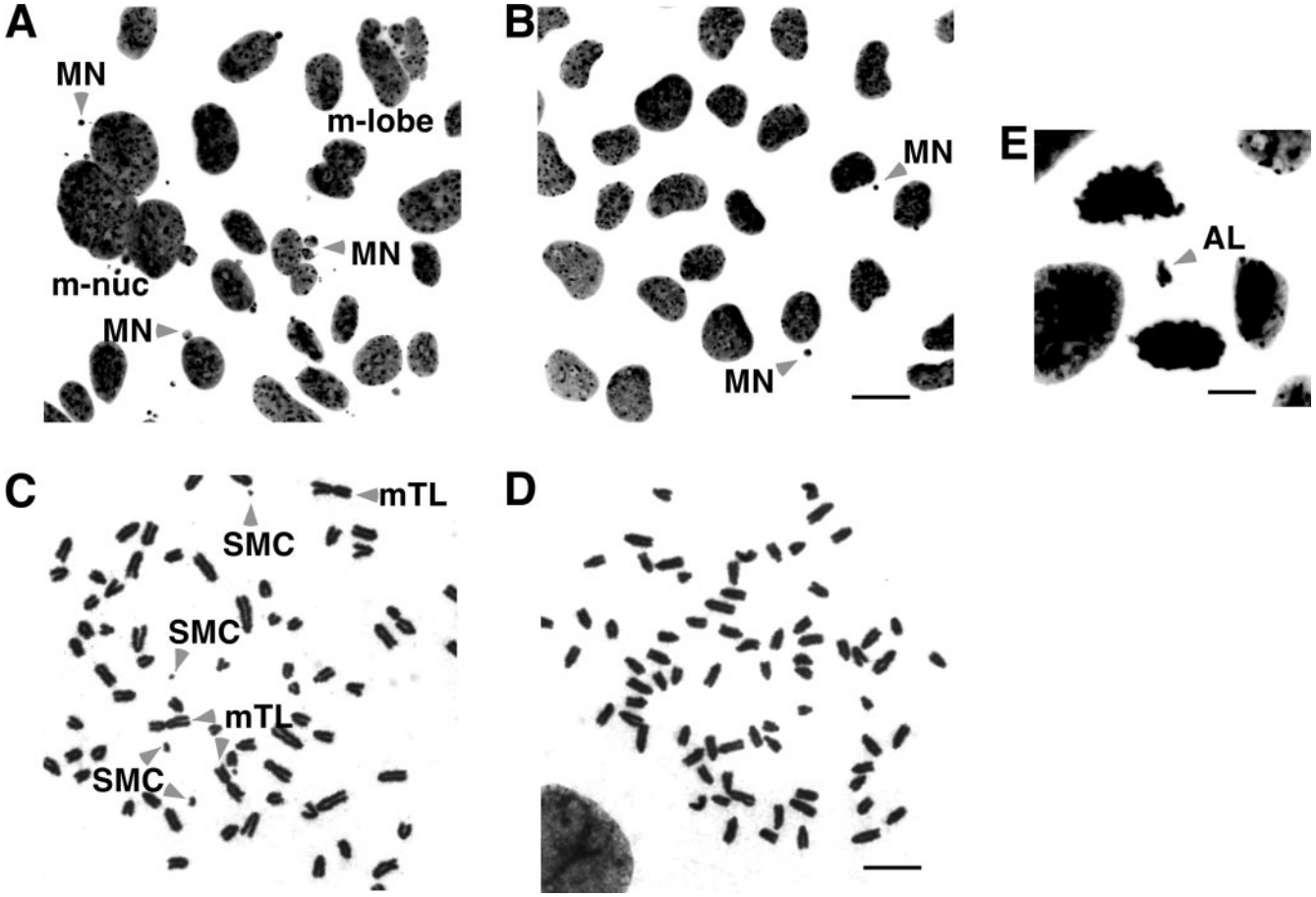

FIG. 4. Nuclear and chromosomal defects are seen in *Blm* mutant mammary tumor cell lines. (A and B) DAPI staining of nuclei obtained from unstable line 1578-2 and stable line 1795-2, respectively. (C and D) Giemsa staining of metaphase spreads from unstable line 9261-9 and stable line 1776-4, respectively. (E) Anaphase figure is seen in DAPI-stained cells from unstable line 1578-2 harvested 2 hours after release from nocodazole arrest. m-nuc, multinucleated; m-lobe, multilobed; mTL, metacentric translocation; SMC, small marker chromosome. Bars, 10 μm.

mation. Panel lines were tested for their transformation potential by anchorage-independent growth assay in soft agar. As shown in Fig. 3E, chromosomally unstable lines 1578-2, 9261-9, and 1579-5, produced the greatest numbers of colonies, whereas stable line 1795-2 and control line 1690-12 produced no colonies among 10^5 cells plated in triplicate per line. In contrast to no growth seen with stable line 1795-2, stable line 1776-4 produced 0.02% ± 0.01% colonies, which is still 15-fold-fewer colonies than the three unstable lines. Similarly, moderately unstable lines 1780-11 and 9354-14 also produced relatively low numbers of colonies (Fig. 3E). As an additional test for neoplastic potential, we evaluated the in vivo growth of the cell lines by subcutaneously injecting cells of various passage numbers derived from each line into nude mice. The frequency and kinetics of tumor growth paralleled those seen with growth in soft agar (data not shown). This growth potential of members of the tumor line panel correlates directly with levels of chromosomal instability and suggests that this instability is the cause of transformation.

Step two: induction of chromosome loss following Cre protein-mediated deletion of *Blm* exon 8. In step two of our cell line analysis protocol, we set out to create the exon 8 deletion mutation in cultured cells with the purpose of determining short-term direct and long-term indirect effects of *Blm* mutation. To produce *Blm* floxed-allele-deleted derivatives from undeleted line 1690-12, we added purified recombinant Cre protein to cells in vitro (40). After cell treatment and expansion of colonies, lines were assayed for deletion of exon 8 by PCR and later validated by Southern blotting (Fig. 2D). We matched nine mutant and nine control subclones and cultured them in parallel for 100 passages, or approximately 1 year, by the 3T3 protocol.

Metaphase spreads obtained from the beginning of the experiment at p4 to p6 were scored for number of chromosomes. The average number of chromosomes per cell was calculated using 200 and 204 metaphases from nine mutant and nine control subclones, respectively. Interestingly, we found an average chromosome loss of 3.8% per cell in mutant cultures relative to control cultures (Fig. 5A). In addition, evaluation of passage 100 metaphase spreads by using 179 and 215 cells from nine mutant and nine control subclones, respectively, showed that the average chromosome loss per cell persisted and increased to 10.6% (Fig. 5B) ($P < 10^{-4}$ in both cases). To confirm the chromosome loss result, additional experiments were performed on derivatives of line 1690-12, subclones U-10 and U-23, and on unrelated floxed-allele-bearing fibrosarcoma

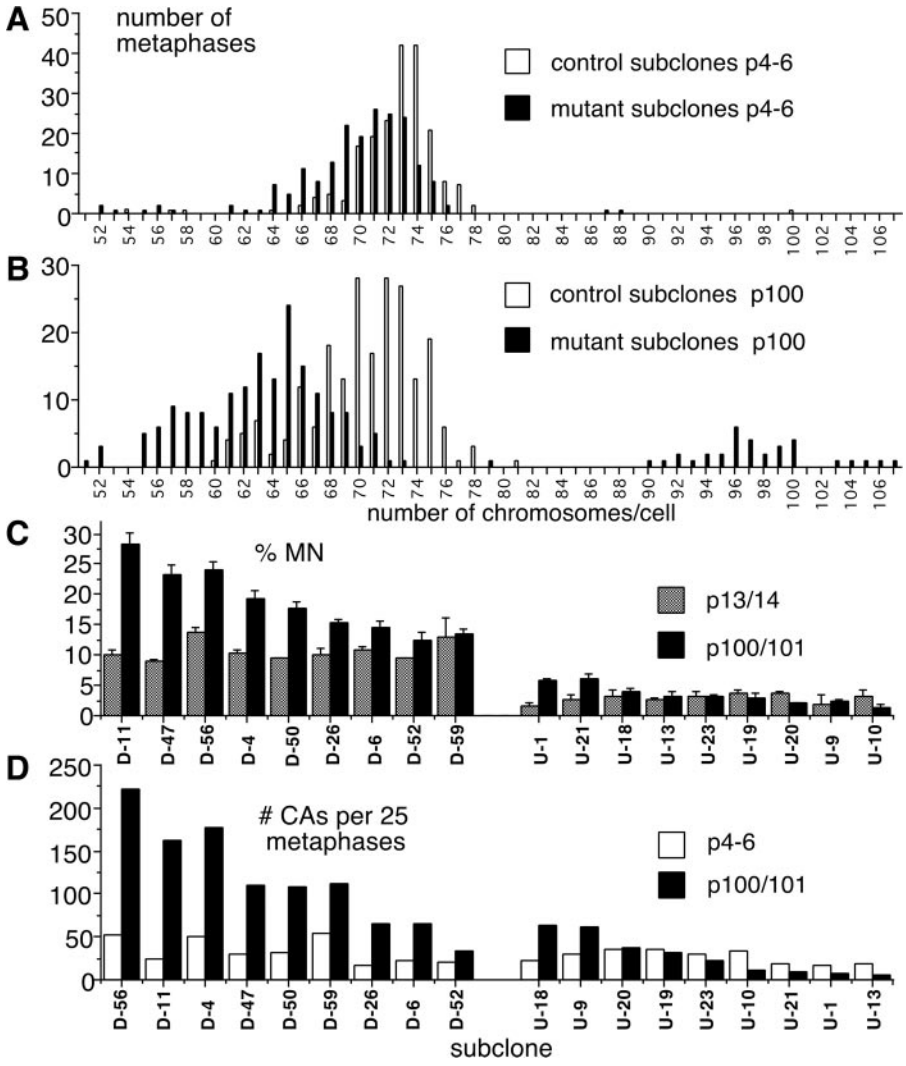

FIG. 5. Time-dependent chromosome loss and increases in numbers of micronuclei and numbers of chromosomal aberrations in mutant subclones obtained from parent line 1690-12. (A) Comparison of numbers of chromosomes/cell in 200 metaphases from nine mutant subclones and 204 metaphases from nine control subclones at the early time point (p4 to p6). (B) Comparison of numbers of chromosomes/cell in 179 metaphases from nine mutant subclones and 215 metaphases from nine control subclones at the late time point (p100). Hypertetraploid cells with numbers of chromosomes varying from 87 to 107 are not included in the chromosome loss calculation. Also, cells with endoreduplicated numbers of chromosomes are not plotted. (C) Comparison of MN at early (p13/14) and late (p100/101) time points for nine mutant (D) and nine control (U) subclones. For each sample, 2×500 cells were scored. Bars represent averages in percent, and error bars indicate standard deviations from the mean. (D) Comparison of numbers of CAs at early (p4 to p6) and late (p100/101) time points for nine mutant (D) and nine control (U) subclones. For each sample, the total number of CAs per 25 metaphases is plotted.

line 9582-5 derived from a tumor in a CKO mouse. Lines U-10, U-23, and 9582-5 produced significant chromosome loss in Cre protein-treated mutant subclones relative to buffer-treated control subclone controls at early passage (averages per cell of 2.0, 3.5, and 5.3%, respectively; $P < 10^{-4}$ in all cases). To control for Cre activity, we added Cre recombinase to NIH 3T3 cells. Subclones from Cre protein-treated NIH 3T3 cells gave an average loss of only 0.2% per cell relative to buffer-treated control subclones. This difference was not significant ($P = 0.52$). Thus, chromosome loss in exon 8-deleted cultures must be mediated by ablation of *Blm* function. Last, we have found significantly more hypodiploid metaphases in cultured primary fibroblasts derived from *Blm* null embryos than in cultures derived from wild-type embryos (data not shown).

Long-term analysis of mutant cell lines reveals induction of time-dependent secondary genomic instability. To determine if mutant subclones had acquired CIN in a time-dependent manner as a consequence of *Blm* mutation, values from beginning and ending time points for both the CA and MN assays were compared. At the first time point, numbers of micronuclei in nine mutant subclones were similar, varying from 9.0 ± 0.3 to 13.8% ± 0.8%. In nine control subclones the range was from 1.5 ± 0.7 to 3.6% ± 0.7% (Fig. 5C, p13/14). The overall difference between the two sets of subclones was approximately fourfold. This confirms induction of the *Blm* mutation phenotype in mutant subclones obtained by Cre protein treatment ($P < 10^{-7}$). At the p100 end time point and after subtraction of p13/14 background values, mutant subclones had

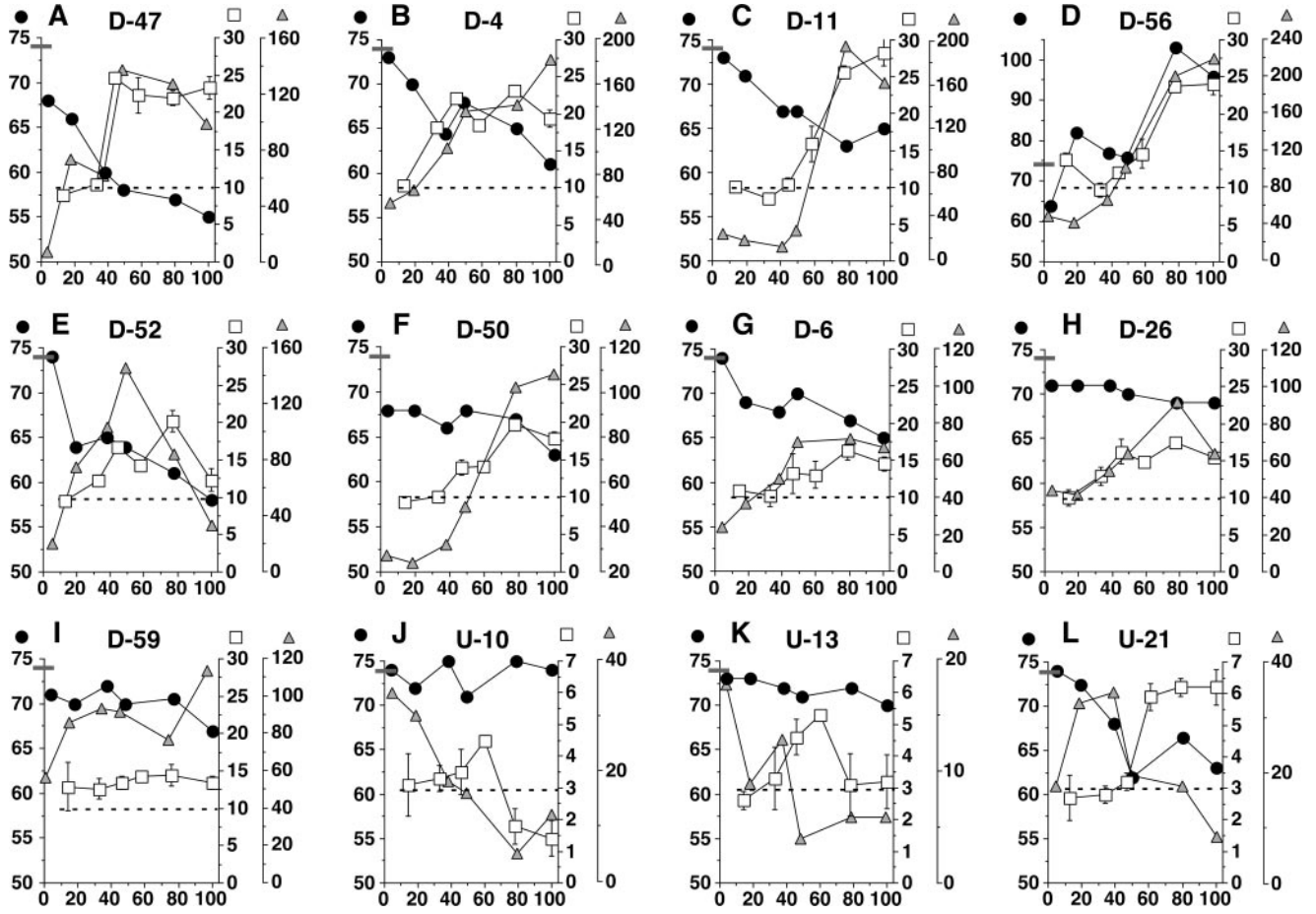

FIG. 6. Acquisition of chromosomal instability is preceded by chromosome loss. Culture history plots are shown for nine mutant (D) and three control (U) subclones from tumor cell line 1690-12. Passage number is plotted on the *x* axis. Three variables are plotted on the *y* axis: modal chromosome number (circles, left axis), MN (squares, innermost right axis), and numbers of CAs (triangles, outermost right axis). The gray bar on the left axis denotes the modal chromosome number of 74 given by parental cell line 1690-12. The dashed line denotes baseline numbers of micronuclei, set at 10% for mutant and 3.0% for control subclones. MN assay results are expressed as the average percentage for 2 × 500 cells scored per time point; error bars are standard deviations from the mean. Modal chromosome number and total number of CAs were determined from 25 metaphases assayed at each time point.

accumulated 72.6 and undeleted subclones 5.7% MN, for a difference of 13-fold (Fig. 5C) ($P = 0.004$). At the beginning p4 to p6 time point, mutant subclones did not produce significantly more structural abnormalities than control subclones, with totals of 304 and 239 CAs, respectively (Fig. 5D; $P = 0.22$). However, at p100, mutant subclones produced 1,057 CAs, compared to 254 CAs for control subclones. After subtraction of p4 to p6 background values, a 50-fold difference in the time-dependent accumulation of CAs was obtained, with 753 and 15 for mutant and control subclones, respectively (Fig. 5D) ($P = 0.001$). Therefore, during the time course, mutant subclones preferentially increase numbers of micronuclei and chromosomal aberrations above those seen in control subclones. These results from the tumor cell line two-step analysis complement one another and allow us to conclude that the CIN present in the unstable members of the original cell panel arises as a result of the *Blm* mutation.

Nonetheless, accumulation of defects in mutant subclones was highly variable for the MN and CA assays (Fig. 5C and D). These wide ranges are reminiscent of what was seen in step one of our two-step protocol and raise the question as to whether these increases occur as a primary or as a secondary consequence of *Blm* mutation. The rather limited ability of early-passage mutant subclones to produce more CAs than are seen in controls argues against mutation in *Blm* being the primary mechanism for producing large numbers of these defects at late passage (Fig. 5D and data not shown). Second, there is no known Bloom's mutation-specific mechanism that would produce variable numbers of micronuclei above baseline levels, nor are micronuclei expected to be heritable.

In two of nine mutant cultures, cell chromosome numbers became hypertetraploid, producing numbers of chromosomes greater than the mouse tetraploid number of 80. For example, mutant subclone D-56 (Fig. 6D) produced a modal number of 64 chromosomes at p4 and a modal hypertetraploid number of 96 chromosomes at p100. In addition, at p100, mutant subclone D-11 (Fig. 6C) produced a modal number of 65 chromosomes, with 8 of 25 metaphases exhibiting values ranging from 92 to 109 chromosomes. Hypertetraploid chromosome numbers are little produced in metaphases from mutant or control sub-

clones at p4 to p6 but appear in mutant and not control subclone metaphases at p100 (Fig. 5A and B). There is no known mechanism by which *Blm* mutation produces these novel chromosome numbers directly. The time dependence of their appearance likely reflects the indirect consequences of loss of the helicase function.

Chromosome loss in mutant subclones is associated with and precedes the appearance of CIN. To better understand how acquisition of time-dependent chromosomal instability occurs, "culture history" plots were generated for mutant and control subclones (Fig. 6). In step one of the analysis, three cell lines were identified as being consistently unstable based on the results of the MN, CA, and AL assays. By the MN assay, unstable lines produced greater than 20% MN, in contrast to the most stable line, which produced a baseline level of 10% MN (Fig. 3B). Therefore, a similar increase was used to distinguish unstable from stable cultures in step two of the analysis. Six of nine mutant (D) cultures increased from a baseline of 10% MN to 20% or greater for a least one time point, qualifying them as unstable. For the four most unstable subclones yielding the highest MN and CA values, there was heterogeneity in time of acquisition of secondary instability. Subclones D-47 and D-4 reached peak values by p44, in contrast to D-11 and D-56, which took longer, reaching peak values by p77 (Fig. 6A to D). For these four subclones and for four of five of the remaining mutant subclones, the kinetics of the increase in numbers of chromosomal aberrations paralleled those of numbers of micronuclei (Fig. 6A to H).

Examination of modal chromosome numbers reveals a time-dependent loss in eight of nine mutant subclones relative to the initial value of 74 chromosomes seen in parental line 1690-12. In the eight mutant subclones, loss was greatest in subclones that were the most unstable and least in the more stable subclones. Subclone D-56 gained chromosomes and, therefore, was excluded from the category of unstable subclones, leaving lines D-47, D-4, D-11, D-52, and D-50, which lost totals of 80, 42, 38, 58, and 44 chromosomes relative to the parent line, respectively (Fig. 6A to C, E, and F). In contrast, the members of the group of more stable subclones, composed of D-6, D-26, and D-59, lost significantly fewer chromosomes, with loss totals of 31, 23, and 24, respectively ($P = 0.01$) (Fig. 6G to I). Examination of the culture histories of two unstable subclones, D-11 and D-50, shows that chromosome loss preceded both the increases in numbers of micronuclei and chromosomal aberrations (Fig. 6C and F). For lines D-47 and D-52, early chromosome loss preceded the upturn in numbers of micronuclei, and in each case this coincided with an early increase in CAs (Fig. 6A and E, respectively). For line D-4, initial chromosome loss coincided with increases in both MN and CAs (Fig. 6B). It is of interest that at the earliest time point, unstable subclone D-56 produced the lowest modal number of chromosomes (64) among the nine mutant subclones. However, this was followed by increases in chromosome numbers as well as MN and CAs during the time course (Fig. 6D). Therefore, on the basis of one time point, D-56 qualifies as having undergone chromosome loss prior to the induction of genomic instability. For none of the six unstable mutant subclones did chromosome loss occur exclusively after the induction of CIN (Fig. 6A to F).

Control subclones (U) lost fewer chromosomes and acquired less genomic instability over their culture histories than did mutant subclones (Fig. 6A to F, J, and K). Unlike mutant cultures, only two of nine control subclones show a twofold, time-dependent increase of micronuclei, with U-21 and U-1 increasing to 6% from a baseline of 3% micronuclei (Fig. 5C and 6L and data not shown). In striking contrast to the case for mutant subclones, the failure of CAs and MN to parallel one another was a typical and different feature of control cultures (Fig. 6J, K, and L and data not shown). In addition, some control subclones appeared to acquire transient genomic instabilities, with U-13, U-9, U-19, and U-23 reaching peaks of approximately 5% micronuclei and declining to baseline levels thereafter (Fig. 6K and data not shown). This contrasts to eight of nine mutant subclones, which tended to sustain higher MN (and CA) values after acquiring them. The sole exception to this is D-52, which acquired a transient instability (compare Fig. 6E to Fig. 6A to D and F to I). Of all control subclones, U-21 showed the most chromosome loss, with a total of 38 lost chromosomes relative to parent line 1690-12. Interestingly, chromosome loss in line U-21 precedes the increase in MN (Fig. 6L). In summary, chromosome loss preceded or coincided with the appearance of instability and occurred to a greater extent in unstable than in stable subclones. This strongly suggests that chromosome loss is a potential mechanism for producing chromosomal instability.

DNA ploidy of mammary tumors in *Blm* conditional knockout mice. Since our results show that the *Blm* mutation can produce chromosomal instability in cultured cell lines, we were interested in determining whether this instability could be detected in vivo in tumor tissue. Nuclei were prepared from sections of fixed mammary tumor samples from *Blm* conditional knockout mice and analyzed by flow cytometry for the appearance of aneuploidy. The myoepithelial tumors that arose in *Hs-cre* and *PSA-cre* female conditional knockout mice consistently yielded diploid DNA contents (Table 1). One exception is tumor sample 9354, which was a combination of three tumor types and exhibited aneuploidy (Table 1). When tumor samples from the *BLG-cre* cohort were analyzed, DNA ploidy differed from that of the previous cohorts, with two aneuploid tumors, four hyperdiploid tumors, and one diploid tumor. One control mouse produced an adenocarcinoma that was aneuploid (Table 1). Human breast cancers typically are of the same types and DNA content ranges as those found in the *Blm BLG-cre* tumor cohort (Table 1) (25). In contrast, adenomyoepithelioma of the breast is a rare and more benign neoplasm appearing in old age (6). Since the lines derived from the *Hs-cre* and *PSA-cre* tumors showed a range of chromosomal instability in culture, we expected to detect aneuploidy in more tumor samples than we did. However, the appearance of aneuploidy in six of seven tumors in the *BLG-cre* cohort provides direct evidence for CIN occurring in vivo in *Blm*-induced neoplasms.

DISCUSSION

From mammary tumors that arose in Bloom's syndrome gene conditional knockout mice, we were able to create a panel of tumor cell lines. From the phenotypes of these lines we sought to determine the relative importances of different forms of genomic instability in producing malignancy in Bloom's syn-

drome. Because the disease predisposes towards the generality of human neoplasia, it is the cancer-related processes that the model recapitulates that are of interest. Thus, insights into the hierarchy of malignancy-associated phenomena such as gene mutation, LOH, aneuploidy, and chromosomal instability in producing neoplasia can be gained.

In the first step of our protocol, members of the panel were subjected to comparative analysis. Results from the SCE assay demonstrated the classic homologous hyperrecombination phenotype. However, unexpected results from additional genomic instability assays on the cell panel led us to the conclusion that some of the tumor cell lines harbored a chromosomal instability in addition to the baseline genomic instability produced by *Blm* mutation (Fig. 3A to D). This additional genomic instability was found to consist of high levels of chromosome missegregation and high numbers of chromosomal structural abnormalities, features that are known to be ubiquitous in human cancers (25, 43). This led further to the question of whether mutation in the Bloom's syndrome gene could produce this CIN.

In the second step of our protocol, we employed a novel time-dependent approach to address the above possibility and found that at least six of nine mutant subclones acquired CIN over a year-long period of culture (Fig. 6A to F). We note that our results differ in this respect from those previously reported (52). However, it was the findings obtained from lines derived from *Blm* mutation-induced tumors that prompted us to employ the nonmutant line as a test reagent in the first place. Additionally, we carried out long-term culture of a number of mutant subclones and controls to measure the indirect effects of the *Blm* mutation. The fact that long culture histories were required to induce CIN raises the question as to what relevant in vivo process is being modeled. Our 3T3 passage protocol utilized cell counting, and we have found that on average each mutant culture accumulated approximately 1×10^9 cells in 100 passages. This number compares favorably to the value of 10^9 cells that a small, 1-cm^3 tumor might contain (16). Therefore, our protocol may serve as a better model for tumor progression than initiation, with mutation in *Blm* destabilizing a preexisting neoplastic lineage prior to its emergence as a clinically relevant tumor.

We observed a consistent predisposition of Bloom's syndrome cells to lose chromosomes. Cultured BS cells produce micronuclei during S phase, and these contain chromosomal material bearing active sites of DNA synthesis as well as centromeres and telomeres (58). We have also been able to document the simultaneous presence of chromosome loss and baseline levels of micronuclei in tumor lines at early times following induction of a *Blm* mutation. A time-dependent decrease in chromosome numbers in mutant subclones is consistent with a constant "chewing" effect on genomes occurring as a consequence of ejection of chromosomal material from the nucleus during the replication cycle (Fig. 5A and B). Chromosome loss has been documented in Bloom's syndrome. For example, a 7-year-old boy and a 31-year-old man showed loss of the Y chromosome in 10% and 15% of peripheral blood lymphocytes, respectively (1, 49). Bone marrow from the boy showed simultaneous loss of the Y chromosome and chromosome 7, associated with myelodysplastic syndrome. The man progressed to acute myeloid leukemia 10 years later, and that malignancy was also associated with loss of both the Y chromosome and chromosome 7 (50). A compilation of karyotypes of nine BS individuals with myelodysplastic syndrome and acute myeloid leukemia revealed that 80% had complete or partial loss of one copy of chromosome 7, versus 5% in the general population with similar cancers (41). In addition, two of three cultured colonic adenomas from a 33-year-old BS man produced cells with a loss of one to three chromosomes (37). Last, mutations in *DmBlm*, the *Drosophila* homolog of human *BLM*, produces germ line chromosome loss (32).

In the second stage of our analysis, we found an association between chromosome loss and induction of CIN in six of nine *Blm* mutant subclones (Fig. 6A to F). These data can be put together in the form of a model in which chromosome loss induces additional genomic instability by introducing insufficiency at the level of single copies of genes. Because it is a large target, the loss of a mammalian chromosome will result in the deletion of a single copy of several hundred to several thousand genes. The six unstable subclones each lost 8 to 14 chromosomes from a starting value of 74 prior to or coinciding with the appearance of secondary instability (Fig. 6A to F). There is precedent for an insufficiency of genes involved in mitosis causing CIN. Haploinsufficiency in Plk4, Bub3, and BubRI and downregulation of MAD1 produce mitotic spindle defects and aneuploidy (8, 29, 30, 31). Our model for Bloom's syndrome-mediated chromosomal instability relies on indirect effects of the *Blm* mutation (Fig. 7). Through loss of multiple chromosomes, gene copy number imbalances are generated and a relatively stable *Blm* mutant cell lineage produces an unstable cell population. This occurs by degrading the ability of cells to assemble a faithful mitotic spindle and maintain proper chromosome architecture (13, 15). Such an unstable state is responsible for producing a range of chromosomal aberrations, including abnormal numbers of chromosomes (hypertetraploidy), chromosome missegregation, and high numbers of structural abnormalities.

Since our evidence that *Blm* mutation produces CIN comes from cultured cell lines, we were interested in determining whether chromosomal instability occurs in vivo in *Blm* mutant tumors. Therefore, we analyzed the DNA contents of tumors produced in the different mouse cohorts. Adenomyoepitheliomas were routinely diploid, in contrast to the adenocarcinomas, which showed a range of DNA contents, with the majority being aneuploid (Table 1). The fact that diploid tumors produced both chromosomally stable and unstable lines suggests that instability could have arisen in culture in members of the cell panel. Alternatively, with the high coefficient of variation found in the myoepithelial tumor samples and with the relative insensitivity of fluorescence-activated cell sorting as an analytical tool, it may not be possible to say whether these tumor samples are genuinely diploid (Table 1). The fact that this difference occurred in mouse raises the question of whether there are substantial karyotype differences in human between the two tumor types. In one study, 10 unselected myoepithelial carcinomas were analyzed by comparative genomic hybridization and yielded a mean of 2.1 DNA copy number changes per genome (28). In another study, 27 adenomyoepithelial tumors were divided into three groups based on increasing malignancy, and when assayed by comparative genomic hybridization they showed means of 2.6, 3.8, and 6.7 copy number

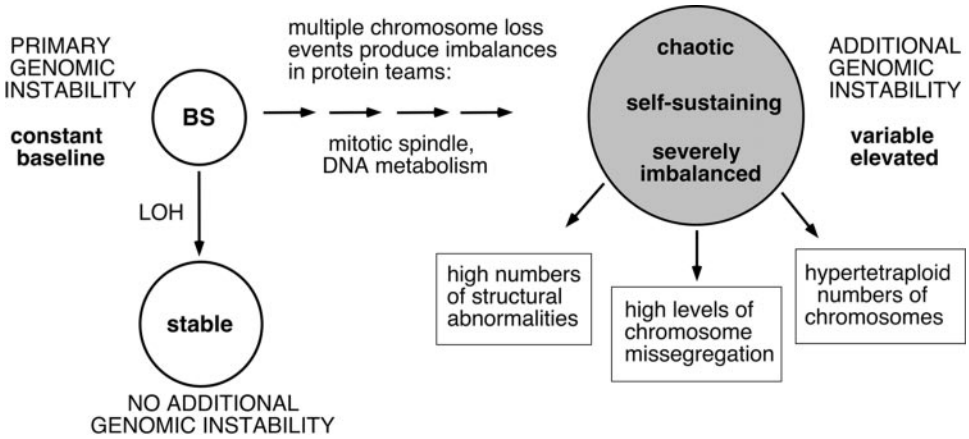

FIG. 7. Model for Bloom's syndrome gene mutation-mediated induction of chromosomal instability. A Bloom's syndrome mutant cell (BS) exhibiting a baseline and constant primary genomic instability evolves into a cell lineage having an additional genomic instability that is variable and elevated. The mechanism of evolution utilizes random, multiple chromosome loss events to produce imbalances in protein teams responsible for proper assembly of the mitotic spindle and maintenance of DNA metabolism. The end result is an unstable cell population bearing a genomic instability that is chaotic, severely imbalanced, and self-sustaining. In contrast, LOH occurring in a BS cell produces a stable lineage without additional genomic instability. The additional genomic instability has the capacity to produce high numbers of chromosomal structural abnormalities, high levels of chromosome missegregation, and hypertetraploid numbers of chromosomes. These abnormalities are characteristic of chromosomal instability.

changes per genome (27). In contrast, in a literature review, the number of alterations found in grade I ductal carcinomas was 5.4 (range of means, 3.6 to 8.0), and this increased to 11.7 in grade III tumors (range of means, 8.4 to 13.8) (28). These reports give evidence that in human, carcinomas are more karyotypically complex than are adenomyoepithial tumors. In addition, regardless of tumor type, there appears to be a strong dependence on tumor grade. The mammary tumors that arose in the three *Blm* Cre cohorts tended to be benign and showed little invasiveness, and metastasis was not seen. These considerations could provide an explanation for the lack of overt DNA content shifts in our adenomyoepitheliomas and for their notable difference from adenocarcinomas.

Very little information exists concerning the karyotype of solid tumors arising in BS individuals. When intestinal adenomas from a BS individual were assayed (37), it was found that four of six polyps had *APC* mutations. Three that were subjected to primary culture and chromosome analysis were mostly diploid. This example has been taken as evidence that Bloom's syndrome hypermutability induces mutations in *APC* that drive the appearance of adenomas while maintaining a cellular diploid state (37, 52). This example is consistent with our DNA content results obtained with adenomyoepitheliomas but not with those obtained with adenocarcinomas.

The results presented here give rise to an alternative hypothesis by which to better understand the increased cancer risk found in Bloom's syndrome. The prevailing view is that hypermutability and LOH induced by hyperrecombination cooperate to unmask mutations in tumor suppressor alleles (18, 21). An increase in loss-of-function mutations in the hypoxanthine phosphoribosyltransferase gene and an increase in frequency of glycophorin A locus variants have been taken as evidence for hypermutability in BS (33, 34, 53, 55). However, the molecular structure of these mutations has not been elucidated, and it remains unclear whether point mutations are involved or if the lesions might be chromosomal in nature. In a mouse model for BS, analysis of a *cII* reporter gene on the *tm3Brd* allele hypomorph (38, 39) background yielded no increase in point mutations or small lesions (54). Additionally, an increase in numbers of micronuclei in mutant reticulocytes versus controls in the same mice was found, supporting the existence of chromosomal events (54). In support of LOH operating on preexisting mutations, heterozygous Apc^{Min} mice developed fourfold more intestinal polyps on the *Blm* hypomorphic versus the wild-type background, with loss of the Apc^{+} allele occurring as a consequence of mitotic recombination with the mutant allele (38). However, loss of a wild-type tumor suppressor allele through recombination between chromosome homologs is predicted to be a weaker form of mutagenesis than loss through chromosome loss. In the case of recombination, the same number of chromosome homologs is retained; however, with chromosome loss all other genes on the chromosome are lost as well. Last, our proposal suggests that it is the acquired chromosomal instability induced by mutation of the Bloom's syndrome gene that has the capacity to remodel the genome at the chromosomal level. The power of this form of mutagenesis resides in its ability to produce defects that are unrelated to the enzymatic activity of the mutated helicase. Indeed, the nature of chromosomal instability is that of a highly disordered state that can allow rapid accumulation of a range of different genetic changes. The chromosomal instability described in this report could provide the genetic plasticity required to drive processes associated with cancer progression. These could include invasion, metastasis, expression of neoantigens, and acquisition of multidrug resistance occurring in advanced malignancies.

ACKNOWLEDGMENTS

We thank Argiris Efstratiadis (Columbia University), Hsiuchen Chen (Caltech), and Christine Watson (University of Cambridge) and John J. Wysolmerski (Yale University) for the *Hs-cre6*, *PSA-cre*, and *BLG-cre* mouse strains, respectively. We acknowledge Anne Har-

rington for ES cell microinjections and Montserrat Michelman and Jen McMenamin for technical assistance. We thank Robert Cardiff (U.C. Davis) and Rod Bronson (Harvard University) for histopathology of mice. Finally, we thank Kevin Freeman for helpful comments on the manuscript.

This work was supported in part by HHMI.

REFERENCES

1. **Aktas, D., A. Koc, K. Boduroglu, G. Hicsonmez, and E. Tuncbilek.** 2000. Myelodysplastic syndrome associated with monosomy 7 in a child with Bloom syndrome. Cancer Genet. Cytogenet. **116:**44–46.
2. **Bachrati, C. Z., and I. D. Hickson.** 2003. RecQ helicases: suppressors of tumorigenesis and premature aging. Biochem. J. **374:**577–606.
3. **Ban, S., T. Shinohara, Y. Hirai, Y. Moritaku, J. B. Cologne, and D. G. MacPhee.** 2001. Chromosomal instability in BRCA1- or BRCA2-defective human cancer cells detected by spontaneous micronucleus assay. Mutat. Res. **474:**15–23.
4. **Cairns, J.** 1981. The origin of human cancers. Nature **289:**353–357.
5. **Chaganti, R. S., S. Schonberg, and J. German.** 1974. A manyfold increase in sister chromatid exchanges in Bloom's syndrome lymphocytes. Proc. Natl. Acad. Sci. USA **71:**4508–4512.
6. **Chang, A., L. Bassett, and S. Bose.** 2002. Adenomyoepithelioma of the breast: a cytologic dilemma. Report of a case and review of the literature. Diagn. Cytopathol. **26:**191–196.
7. **Chester, N., F. Kuo, C. Kozak, C. D. O'Hara, and P. Leder.** 1998. Stage-specific apoptosis, developmental delay, and embryonic lethality in mice homozygous for a targeted disruption in the murine Bloom's syndrome gene. Genes Dev. **12:**3382–3393.
8. **Dai, W., Q. Wang, T. Liu, M. Swamy, Y. Fang, S. Xie, R. Mahmood, Y. M. Yang, M. Xu, and C. V. Rao.** 2004. Slippage of mitotic arrest and enhanced tumor development in mice with BubR1 haploinsufficiency. Cancer Res. **64:**440–445.
9. **Davies, S. L., P. S. North, A. Dart, N. D. Lakin, and I. D. Hickson.** 2004. Phosphorylation of the Bloom's syndrome helicase and its role in recovery from S-phase arrest. Mol. Cell. Biol. **24:**1279–1291.
10. **Dietrich, P., I. Dragatsis, S. Xuan, S. Zeitlin, and A. Efstratiadis.** 2000. Conditional mutagenesis in mice with heat shock promoter-driven cre transgenes. Mamm. Genome **11:**196–205.
11. **Dressler, L. G., and D. Visscher.** 1997. Isolation of nuclei from paraffin-embedded tissue, p. 5.2.9–5.2.15. *In* J. P. Robinson, Z. Darzynkiewicz, P. Dean, O. Alberto, P. Rabinovitch, C. C. Stewart, H. Tanke, and L. Wheeless (ed.), Current protocols in cytometry, Wiley and Sons, New York, N.Y.
12. **Duesberg, P., and D. Rasnick.** 2000. Aneuploidy, the somatic mutation that makes cancer a species of its own. Cell Motil. Cytoskeleton **47:**81–107.
13. **Duesberg, P., and R. Li.** 2003. Multistep carcinogenesis: a chain reaction of aneuploidizations. Cell Cycle **2:**202–210.
14. **Ellis, N. A., J. Groden, T.-Z. Ye, J. Straughen, D. J. Lennon, S. Ciocci, M. Proytcheva, and J. German.** 1995. The Bloom's syndrome gene product is homologous to RecQ helicases. Cell **83:**655–666.
15. **Fabarius, A., R. Hehlmann, and P. H. Duesberg.** 2003. Instability of chromosome structure in cancer cells increases exponentially with degrees of aneuploidy Cancer Genet. Cytogenet. **143:**59–72.
16. **Friberg, S., and S. Mattson.** 1997. On the growth rates of human malignant tumors: implications for medical decision making. J. Surg. Oncol. **65:**284–297.
17. **German, J., R. Archibald, and D. Bloom.** 1965. Chromosomal breakage in a rare and probably genetically determined syndrome of man. Science **148:**506–507.
18. **German, J.** 1993. Bloom syndrome: a mendelian prototype of somatic mutational disease. Medicine (Baltimore) **72:**393–406.
19. **German, J., and B. Alhadeff.** 1994. Analysis of sister-chromatid exchanges, p. 8.6.1-8.6.10. *In* N. C. Dracopoli, J. L. Haines, B. R. Korf, D. T. Moir, C. C. Morton, C. E. Seidman, J. G. Seidman, and D. R. Smith (ed.), Current protocols in human genetics, vol. 1. Wiley and Sons, New York, N.Y.
20. **German, J.** 1997. Bloom's syndrome. XX. The first 100 cancers. Cancer Genet. Cytogenet. **93:**100–106.
21. **German, J.** 2004. Constitutional hyperrecombinability and its consequences. Genetics **168:**1–8.
22. **Hand, R., and J. German.** 1975. A retarded rate of DNA chain growth in Bloom's syndrome. Proc. Natl. Acad. Sci. USA **72:**758–762.
23. **Harvey, M., A. T. Sands, R. S. Weiss, M. E. Hegi, R. W. Wiseman, P. Pantazis, B. C. Giovanella, M. A. Tainsky, A. Bradley, and L. A. Donehower.** 1993. *In vitro* growth characteristics of embryo fibroblasts isolated from p53-deficient mice. Oncogene **8:**2457–2467.
24. **Heartlein, M. W., H. Tsuji, and S. A. Latt.** 1987. 5-Bromodeoxyuridine-dependent increase in sister chromatid exchange formation in Bloom's syndrome is associated with reduction in topoisomerase II activity. Exp. Cell Res. **169:**245–254.
25. **Heim, S., and F. Mitelman.** 1995. Cancer cytogenetics: chromosomal and molecular genetic aberrations of tumor cells, 2nd ed., p. 369–387. Wiley-Liss, New York, N.Y.
26. **Honma, M., S. Tadokoro, H. Sakamoto, H. Tanabe, M. Sugimoto, Y. Furuichi, T. Satoh, T. Sofuni, M. Goto, and M. Hayashi.** 2002. Chromosomal instability in B-lymphoblasotoid cell lines from Werner and Bloom syndrome patients. Mutat. Res. **520:**15–24.
27. **Hungermann, D., H. Buerger, C. Oehlschlegael, H. Herbst, and W. Boecker.** 2005. Adenomyoepithelial tumours and myoepithelial carcinomas of the breast—a spectrum of monophasic and biphasic tumours dominated by immature myoepithelial cells. BMC Cancer **5:**92.
28. **Jones, C., M. P. Foschini, R. Chagger, Y.-J. Lu, D. Wells, J. M. Shipley, V. Eusebi, and S. R. Lakhani.** 2000. Comparative genomic hybridization analysis of myoepithelial carcinoma of the breast. Lab. Investig. **80:**831–836.
29. **Kalitsis, P., K. J. Fowler, B. Griffiths, E. Earle, C. W. Chow, K. Jamsen, and K. H. Choo.** 2005. Increased chromosome instability but not cancer predisposition in haploinsufficient Bub3 mice. Genes Chromosomes Cancer **44:**29–36.
30. **Kienitz, A., C. Vogel, I. Morales, R. Muller, and H. Bastians.** 2005. Partial downregulation of MAD1 causes spindle checkpoint inactivation and aneuploidy, but does not confer resistance towards taxol. Oncogene **24:**4301–4310.
31. **Ko, M. A., C. O. Rosario, J. W. Hudson, S. Kulkarni, A. Pollett, J. W. Dennis, and C. J. Swallow.** 2005. Plk4 haploinsufficiency causes mitotic infidelity and carcinogenesis. Nat. Genet. **37:**883–888.
32. **Kusano, K., D. M. Johnson-Schlitz, and W. R. Engels.** 2001. Sterility of *Drosophila* with mutations in the Bloom syndrome gene—complementation by Ku70. Science **291:**2600–2602.
33. **Kyoizumi, S., N. Nakamura, H. Takebe, K. Tatsumi, J. German, and M. Akiyama.** 1989. Frequency of variant erythrocytes at the glycophorin-A locus in two Bloom's syndrome patients. Mutat. Res. **214:**215–222.
34. **Langlois, R. G., W. L. Bigbee, R. H. Jensen, and J. German.** 1989. Evidence for increased in vivo mutation and somatic recombination in Bloom's syndrome. Proc. Natl. Acad. Sci. USA **86:**670–674.
35. **Lengauer, C., K. W. Kinzler, and B. Vogelstein.** 1998. Genetic instabilities in human cancers. Nature **396:**643–649.
36. **Lonn, U., S. Lonn, U. Nylen, G. Winblad, and J. German.** 1990. An abnormal profile of DNA replication intermediates in Bloom's syndrome. Cancer Res. **50:**3141–3145.
37. **Lowy, A. M., J. J. Kordich, V. Gismondi, L. Varesco, R. I. Blough, and J. Groden.** 2001. Numerous colonic adenomas in an individual with Bloom's syndrome. Gastroenterology **121:**435–439.
38. **Luo, G., I. M. Santoro, L. D. McDaniel, M. Mills, I. Nishijima, H. Youssoufian, H. Vogel, R. A. Schultz, and A. Bradley.** 2000. Cancer predisposition caused by elevated mitotic recombination in Bloom mice. Nat. Genet. **26:**424–429.
39. **McDaniel, L. D., N. Chester, M. Watson, A. D. Borowsky, P. Leder, and R. A. Schultz.** 2003. Chromosome instability and tumor predisposition inversely correlate with BLM protein levels. DNA Repair (Amsterdam) **2:**1387–1404.
40. **Peitz, M., K. Pfannkuche, K. Rajewsky, and F. Edenhofer.** 2002. Ability of the hydrophobic FGF and basic TAT peptides to promote cellular uptake of recombinant Cre recombinase: a tool for efficient genetic engineering of mammalian genomes. Proc. Natl. Acad. Sci. USA **99:**4489–4494.
41. **Poppe, B., H. Van Limbergen, N. Van Roy, E. Vandecruys, A. De Paepe, Y. Benoit, and F. Speleman.** 2001. Chromosomal aberrations in Bloom syndrome patients with myeloid malignancies. Cancer Genet. Cytogenet. **128:**39–42.
42. **Rabinovitch, P. S.** 1994. DNA content histogram and cell-cycle analysis. Methods Cell Biol. **41:**263–296.
43. **Rajagopalan, H., and C. Lengauer.** 2004. Aneuploidy and cancer. Nature **432:**338–341.
44. **Rajagopalan, H., P. V. Jallepalli, C. Rago, V. E. Velculescu, K. W. Kinzler, B. Vogelstein, and C. Lengauer.** 2004. Inactivation of hCDC4 can cause chromosomal instability. Nature **428:**77–81.
45. **Rosin, M. P., and J. German.** 1985. Evidence for chromosome instability *in vivo* in Bloom syndrome: increased numbers of micronuclei in exfoliated cells. Hum. Genet. **71:**187–191.
46. **Schroeder, T. M., and J. German.** 1974. Bloom's syndrome and Fanconi's anemia: demonstration of two distinctive patterns of chromosome disruption and rearrangement. Humangenetik **25:**299–306.
47. **Selbert, S., D. J. Bentley, D. W. Melton, D. Rannie, P. Lourenco, C. J. Watson, and A. R. Clarke.** 1998. Efficient BLG-Cre mediated gene deletion in the mammary gland. Transgenic Res. **7:**387–396.
48. **Sieber, O. M., K. Heinimann, and I. P. Tomlinson.** 2003. Genomic instability—the engine of tumorigenesis? Nat. Rev. Cancer **3:**701–708.
49. **Shabtai, F., and I. Halbrecht.** 1980. Bloom's syndrome, missing Y, hypogonadism and cancer. Clin. Genet. **18:**93–95.
50. **Shabtai, F., U. H. Lewinski, A. Meroz, D. Klar, M. Djaldetti, and I. Halbrecht.** 1988. Non-random chromosomal aberrations in a complex leukaemic clone of a Bloom's syndrome patient. Hum. Genet. **80:**311–314.
51. **Shiraishi, Y., and A. A. Sandberg.** 1977. The relationship between sister chromatid exchanges and chromosome aberrations in Bloom's syndrome. Cytogenet. Cell. Genet. **18:**13–23.
52. **Traverso, G., C. Bettegowda, J. Kraus, M. R. Speicher, K. W. Kinzler, B. Vogelstein, and C. Lengauer.** 2003. Hyper-recombination and genetic instability in BLM-deficient epithelial cells. Cancer Res. **63:**8578–8581.

53. **Vijayalaxmi, H. J. Evans, J. H. Ray, and J. German.** 1983. Bloom's syndrome: evidence for an increased mutation frequency in vivo. Science **221:** 851–853.
54. **Wang, Y., and J. A. Heddle.** 2004. Spontaneous and induced chromosomal damage and mutations in Bloom Syndrome mice. Mutat. Res. **554:**131–137.
55. **Warren, S. T., R. A. Schultz, C.-C. Chang, M. H. Wade, and J. E. Trosko.** 1981. Elevated spontaneous mutation rate in Bloom syndrome fibroblasts. Proc. Natl. Acad. Sci. USA **78:**3133–3137.
56. **Wu, L., S. L. Davies, P. S. North, H. Goulaouic, J. F. Riou, H. Turley, K. C. Gatter, and I. D. Hickson.** 2000. The Bloom's syndrome gene product interacts with topoisomerase III. J. Biol. Chem. **275:**9636–9644.
57. **Wu, L., and I. D. Hickson.** 2003. The Bloom's syndrome helicase suppresses crossing over during homologous recombination. Nature **426:**870–874.
58. **Yankiwski, V., R. A. Marciniak, L. Guarente, and N. F. Neff.** 2000. Nuclear structure in normal and Bloom syndrome cells. Proc. Natl. Acad. Sci. USA **97:**5214–5219.